An Iterative Planning Method with Dual-Loop Adaptive Representative Scenario Update for Multi-Area Asynchronously Interconnected Grids

Zhuoyuan Yong
Department of Electrical Engineering
Tsinghua University
Beijing 100084, China
yongzy21@mails.tsinghua.edu.cn

Yiliu He
Department of Electrical Engineering
Tsinghua University
Beijing 100084, China
he-yl21@mails.tsinghua.edu.cn

Haiwang Zhong
Department of Electrical Engineering
Tsinghua University
Beijing 100084, China
zhonghw@tsinghua.edu.cn

***Abstract*—The rapid growth of renewable generation and the increasing adoption of multi-area asynchronously interconnected grids have introduced new challenges for system planning. Conventional planning methods relying on fixed representative scenarios often fail to capture operating conditions across diverse regions. This paper proposes an iterative planning method with dual-loop adaptive representative scenario update. A centralized planning model is developed that co-optimizes generation, transmission and storage. Typical scenarios are derived via operational-state-based clustering, while extreme scenarios are identified via a targeted selection strategy based on multi-time-scale indicators. The iterative framework links planning, operation simulation and scenario update with a dual-loop mechanism, allowing representative scenarios to be dynamically refined. The case study on a modified RTS-GMLC system demonstrates that the proposed method can effectively identify extreme scenarios to ensure the feasibility of planning schemes while enhancing economic performance with acceptable computational effort.**

***Index Terms*—power system planning, dual-loop adaptive representative scenario update, iterative framework, multi-area asynchronously interconnected grid**

I. Introduction

With the widespread deployment of HVDC forming multi-area asynchronously interconnected grids (MAIGs), planning must shift toward centralized coordination, which is a large-scale optimization problem. To improve computational efficiency, typical scenarios are often extracted for the operation simulation of planning. While typical patterns are dominated by seasonal hydropower and load variations in traditional systems, high renewable penetration has made operational states more diverse. Many studies therefore apply statistical or unsupervised learning methods to identify typical scenarios. For example, K-means and hierarchical clustering are applied respectively in [1] and [2], while reference [3] incorporates multiple indicators into a scenario-based programming formulation. However, these methods rely solely on boundary conditions such as renewable output and load levels, failing to reveal the true operational characteristics of the system.

This work was supported by the National Natural Science Foundation of China under Grant U22B6007.

Meanwhile, the growing variability and uncertainty of renewable generation highlight the need to include more targeted extreme scenarios in planning. In [4], extreme scenarios are identified through physical interpretation and expert judgment. In [5], the maximum difference algorithm is used to extract extreme scenarios. In [6], net-load extreme days are incorporated into selection with additional weighting. These studies rely on a single metric, lacking a structured indicator system for defining extreme scenarios. Besides, most scenario extraction methods fix scenarios before planning and therefore ignore how planning decisions influence representativeness.

In addition, existing methods cannot identify all extreme scenarios in advance to ensure planning feasibility. To address this, an iterative feasibility-enforcing method is adopted in [7], which continually identifies infeasible scenarios through operation simulation and adds all of them as new extreme scenarios, re-planning the system until feasibility is ensured across all scenarios. However, this method remains open-loop regarding economic representativeness, and the simultaneous addition of all infeasible scenarios causes significant constraint redundancy, reducing computational efficiency.

In summary, traditional methods are insufficient in facing MAIG's physical complexities. First, they fail to capture frequency security risks arising from asynchronous partitions based on boundary conditions. Second, static scenario selection misses the complex heterogeneity and strong regional coupling, failing to reflect how planning decisions influence the operational state. Finally, existing methods struggle to balance multi-dimensional objectives, often sacrificing economic representativeness or security assurance to avoid computational intractability, particularly in large-scale MAIGs.

To address these challenges, this paper proposes an iterative planning method with dual-loop adaptive representative scenario update for MAIG. The main contributions are as follows:

- A centralized MAIG planning model is developed that co-optimizes generation, transmission and storage across all interconnected areas.
- A representative scenario extraction method is proposed. Typical scenarios are identified through operational-state-

979-8-3315-8138-1

based clustering, while extreme scenarios are selected using physics-based indicators defined over multiple time scales, including sustained low renewable output, short-term reserve adequacy, and transient frequency security.

- An iterative framework is established. By coupling the dual-loop adaptive update of typical and extreme scenarios, the framework effectively bridges planning and operation, achieving a coordinated balance between economic representativeness, security, and computational efficiency.

II. Centralized MAIG planning model

A. Objective Function

The centralized MAIG planning model is established to minimize the total annualized cost, as shown in (1).

$$\min\ C_{\text{inv}} + C_{\text{mat}} + C_{\text{op}} \tag{1}$$

The annualized investment cost C_{inv} is shown in (2), where r is the discount rate and N is the device lifespan.

$$C_{\text{inv}} = C_{\text{inv}}^{\text{total}} \cdot \frac{(1+r)^N - 1}{r(1+r)^N} \tag{2}$$

The total investment cost $C_{\text{inv}}^{\text{total}}$ is given by (3), which aggregates costs for generation, transmission and storage.

$$\begin{aligned} C_{\text{inv}}^{\text{total}} = &\sum_{g\in\mathcal{G}} C_g^{\text{G,I}}\, \overline{p}_g^{G,I} + \sum_{l\in\mathcal{L}} C_l^{\text{L,I}}\, \overline{p}_l^{L,I} \\ &+ \sum_{es\in\mathcal{ES}} \left(C_{es}^{\text{ES,I,C}}\, \overline{p}_{es}^{ES,I} + C_{es}^{\text{ES,I,S}}\, \overline{e}_{es}^{ES,I} \right) \end{aligned} \tag{3}$$

The annual maintenance cost C_{mat} represents the annual expenses required to ensure the reliable operation of existing assets. It is assumed to be proportional to the installed capacities of the devices, consistent with the formulation of $C_{\text{inv}}^{\text{total}}$.

The annual operational cost C_{op} is given by (4), where π_s denotes the probability of scenario s, $C_g^{\text{G,O}}$ is the variable generation cost, and $C_g^{\text{G,SU}}$ represents the start-up cost of thermal units.

$$C_{\text{op}} = \sum_{s\in\mathcal{S}} \pi_s \sum_{t\in\mathcal{T}} \sum_{g\in\mathcal{G}} \left(C_g^{\text{G,O}}\, p_{s,g,t}^{G} + C_g^{\text{G,SU}}\, \overline{p}_{s,g,t}^{SU} \right) \tag{4}$$

B. Constraints

The constraints of the model are divided into two categories: planning constraints and operational constraints under representative scenarios. Most of them have been described in [8] and therefore are not repeated here. A complete summary of the constraints adopted in this study is provided in Table I.

TABLE I
Constraints of the planning model

Constraint	Description
Planning constraints	
Installed capacity	Maximum construction of devices
Carbon emissions	Emission cap for the planning horizon
Operational constraints under representative scenarios	
Power balance	Nodal supply–demand balance
Power flow	AC transmission line thermal limits
Spinning reserve	Reserve requirement under renewable variability
Frequency security	Nadir, RoCoF, and steady-state deviation
Thermal unit operation	Power output, minimum online/offline time, and ramping constraints
Renewable generation	Upper bounds on renewable output
Storage operation	Charging/discharging power, energy capacity, and intertemporal energy balance
HVDC operation	DC transmission limits

The HVDC line is modeled by virtual generators at terminal nodes, whose equal-magnitude and opposite-direction outputs represent injection and withdrawal. The DC transmitted power is constrained by (5), where $p_{s,l,t}^{DC}$ denotes the DC power, with $\underline{P}_l^{DC}$ and $\overline{P}_l^{DC}$ as the minimum and maximum limits.

$$\underline{P}_l^{DC} \le p_{s,l,t}^{DC} \le \overline{P}_l^{DC}, \quad \forall\, s,\, l,\, t \tag{5}$$

In conventional planning, unit-commitment-based operation introduces numerous binary variables, leading to combinatorial explosion under multi-scenario, time-coupled conditions. This study replaces binary commitment decisions with continuous online generation capacity, following the formulation in [8].

The system frequency response is described using the aggregated system frequency response model in [9]. The relationship between the power imbalance $\Delta P(s)$ and the resulting frequency deviation $\Delta f(s)$ is given by (6). The frequency response parameters are assumed to be proportional to the continuous online generation capacity.

$$\Delta P(s) = \left(2Hs + D + \frac{1 + F_H T_R s}{R(1+T_R s)} \right) \Delta f(s) \tag{6}$$

For a sudden imbalance $\Delta P(s) = \Delta P_L / s$, the frequency nadir Δf_{nadir} is a nonlinear function. To embed this nonlinear constraint into the planning model, a piecewise-linear approximation is constructed. Let $\boldsymbol{X} = [H, D, 1/R, F_H/R]$ and $h(\boldsymbol{X}) = \Delta P_L / \Delta f_{nadir}$. A dataset $(\boldsymbol{X}_n, y_n)$ is generated by $y = h(\boldsymbol{X})$. Multiple linear segments $\left(\boldsymbol{\alpha}_{(k)}, \beta_{(k)}\right)$ are then fitted to this dataset through a least-squares procedure, resulting in a set of affine functions that collectively approximate the original mapping.

This study addresses MAIG frequency security under severe power deficits caused by HVDC $N-1$ blocking contingencies. The linearized frequency nadir constraint is given by (7), where Δf_{lim} denotes the allowable frequency nadir limit.

$$\boldsymbol{\alpha}_{(k)}^T \boldsymbol{X}^{s,t} + \beta_{(k)} \ge \frac{p_{s,l,t}^{DC}}{\Delta f_{\text{lim}}}, \quad \forall s,\, l,\, t \tag{7}$$

III. Representative Scenario Extraction Method Considering Operational States

A. Definition of Representative Scenario and Traditional Extraction Method Based on Boundary Conditions

To reduce the computational burden of planning, representative scenarios, including typical ones for economic assessment and extreme ones for security and feasibility, are used for operation simulation.

Traditional approaches obtain typical scenarios by clustering boundary conditions such as renewable and load time series.

979-8-3315-8138-1

The K-Medoids algorithm is widely used, selecting the actual sample closest to each cluster center as the medoid.

A commonly used dissimilarity-based approach extracts extreme scenarios by iteratively selecting the case farthest from the existing scenario set. In each iteration, the scenario most distant from the current typical and previously selected extreme scenarios is chosen, and the process continues until the required number of extreme scenarios is obtained.

B. Typical Scenario Clustering Based on Operational States

Breaking through the traditional clustering that focuses on boundary conditions, this study proposes a data-driven method for typical scenario clustering based on system operational states. The detailed algorithm is as follows:

1) Construction of the Operational State Vector: The operational state vector $\mathbf{v}$ is defined by (8) to capture MAIG's operational characteristics, where $\mathbf{o}_{|G_{TG}|\times T}$ is the on/off status of thermal units, $\mathbf{g}_{|G|\times T}$ is generator power output, $\mathbf{f}_{|F|\times T}$ is AC transmission line power flows, $\mathbf{es}_{|ES|\times T}$ is the charging and discharging power of storage, and $\mathbf{dc}_{|DC|\times T}$ is HVDC transmission power. Linearly dependent variables (e.g., nodal loads) are excluded to reduce dimensionality and focus on controllable decision variables.

$$\mathbf{v} = \left(\mathbf{o}_{|G_{TG}|\times T}, \mathbf{g}_{|G|\times T}, \mathbf{f}_{|F|\times T}, \mathbf{es}_{|ES|\times T}, \mathbf{dc}_{|DC|\times T}\right)^{\mathrm{T}} \quad (8)$$

2) Dimensionality Reduction: Due to the high dimensionality of operational data, PCA (Principal Component Analysis) is then used to obtain an uncorrelated low-dimensional representation. The first k principal components are retained based on cumulative variance, providing a compact representation of the operational states.

3) Clustering: Typical scenarios are obtained by applying K-Medoids clustering in the reduced feature space. By grouping operational states according to similarities in key features and selecting cluster medoids as representatives, this approach produces a compact scenario set for planning.

C. Extreme Scenario Selection Based on Physical Indicators Defined over Multiple Time Scales

As high-dimensional operational states do not directly reveal feasibility-critical behavior, this study introduces physics-based security indicators to identify extreme scenarios more effectively. A selection method based on indicators defined over multiple time scales is developed, integrating sustained low renewable output, short-term reserve adequacy, and transient frequency security. Together, these indicators characterize a wide range of extreme operating conditions.

1) Sustained Low Renewable Output: When the renewable power ξ_d remains below a fraction α of its daily maximum $\xi^{\max}$ for several continuous days [10], the system must rely on thermal units and storage to maintain net-load balance over a long horizon. Let d_1 and d_2 denote the start and end of the period. If $\xi_d \le \alpha\xi^{\max}$ for all $d_1 \le d \le d_2$ and $d_2 - d_1 \ge \delta$, this interval is identified as a sustained low renewable output scenario. The severity is measured by the index γ, defined as the ratio of the cumulative net-load generation deficit to the total net load over the interval, as shown in (9).

$$\gamma = 1 - \left(\int_{d_1}^{d_2} \xi_d \,\mathrm{d}t\right) \Big/ \left(\sum_{d=d_1}^{d_2}\sum_{t=1}^{|\mathcal{T}|}\sum_{n=1}^{|\mathcal{N}|} D_{n,d,t}\right) \quad (9)$$

2) Short-term Reserve Adequacy: In each area of MAIG, the available reserve capacity reflects its short-term capability to cope with load and renewable generation fluctuations. As each area depends mainly on its own reserves and receives support via HVDC links, assessing the combined reserve capability of internal resources and HVDC support is necessary. Based on the spinning reserve constraints, the reserve supply and demand of area a are denoted by P_a^{s} and P_a^{d}. The reserve margin indicator μ_a is defined by (10).

$$\mu_a = \frac{P_a^{\mathrm{d}} - P_a^{\mathrm{s}}}{P_a^{\mathrm{d}}} \quad (10)$$

3) Transient Frequency Security: HVDC blocking can cause severe frequency drops in MAIG, making it essential to assess each area's ability to withstand such disturbances. This study uses the frequency nadir $\Delta f_a^{\mathrm{nadir}}$ under the worst HVDC blocking event as the extreme indicator.

Based on the three indicators, a targeted selection strategy is established to identify extreme scenarios: Infeasible operation scenarios are first collected as candidates, after which all indicators are computed and normalized to ensure comparability. Each scenario is then mapped into an indicator space, where the distance of its indicator vector from the origin is computed as the combined severity measure. Since larger indicator values imply more extreme conditions, scenarios farther from the origin are judged more extreme and finally selected.

IV. Iterative Framework with Dual-Loop Adaptive Representative Scenario Update

A. Iteration Process

With the MAIG planning model and scenario extraction method established, this section proposes an iterative planning framework with dual-loop adaptive representative scenario update. The iteration process is shown in Fig. 1.

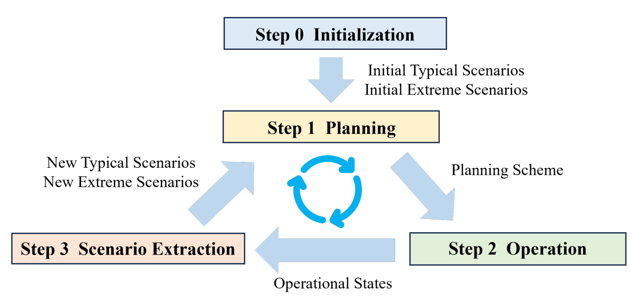

Fig. 1. The iteration process of the framework.

1) Initialization: Since no operation results are available at the beginning of the iterative process, the renewable–load–based scenario extraction method in Section III-A is used to generate the initial representative scenarios.

979-8-3315-8138-1

2) Planning: The centralized MAIG planning model in Section II is solved to obtain an updated planning scheme.

3) Operation: Based on the planning scheme, an operation simulation is conducted. The objective and most constraints remain consistent with the planning model, except that unit commitment is restored. Since the scenario extraction methods proposed in this study require feasible operational states, the power-balance constraint is relaxed with load-shedding slack variables, and a large penalty is added to the objective to ensure that load shedding occurs only when no feasible solution exists otherwise.

4) Scenario extraction: Using the operation results, typical and extreme scenarios are extracted following the method in Section III-B and III-C, which are then provided to the planning model for the next iteration.

The cycle continues until the operation results of all scenarios are feasible, at which point the iteration process converges.

B. Dual-Loop Adaptive Representative Scenario Update

Building on the scenario extraction methods proposed in this study, this section develops a dual-loop adaptive representative scenario update procedure, as shown in Fig. 2.

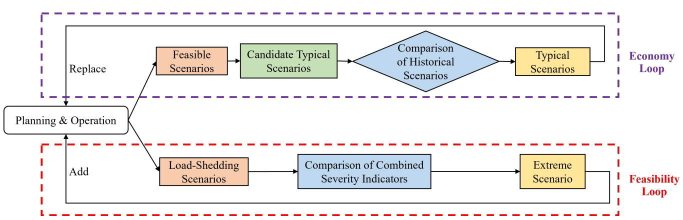

Fig. 2. The dual-loop adaptive representative scenario update procedure.

In the economy loop, typical scenarios are selected from feasible ones to ensure the economic representativeness. To balance representativeness and computational efficiency, the weekly timescale is adopted, and the number of scenarios is determined based on the marginal gain of operational cost representativeness, identifying the knee point of the operational cost error curve versus scenarios number (4 in this study), where accuracy gains diminish significantly relative to the rising computational burden. In each iteration, the typical scenarios are adaptively updated, selecting the set that best matches the actual operational cost from historical set for the next planning step.

In the feasibility loop, extreme scenarios are included to ensure the security of the planning scheme. All load-shedding scenarios serve as natural candidates, from which the selection method in Section III-C identifies the most severe cases. The number of added extreme scenarios balances convergence rate against computational burden, and a small value (1 in this study) is recommended for large-scale systems to fully exploit the iterative adaptability, enabling the dynamic identification of feasibility-critical risks without redundancy. This prevents constraint explosion and ensures the master problem remains computationally tractable.

Finally, the optimality and convergence of the iterative framework are analyzed. Each iteration selects a typical scenario set, which is no less economically representative than that of the previous round. Although representative scenarios cannot guarantee a global optimum, the iterative updates progressively improve the solution quality. For convergence, each iteration adds the extreme scenario without removal, causing the extreme scenario set to grow and the feasible region to shrink monotonically. As the scenario set is finite, the iterative model converges in finite steps.

Table II summarizes the key distinctions and novelties of this study relative to existing scenario-based planning methods.

TABLE II
COMPARISON OF SCENARIO-BASED PLANNING METHODS

Method	Open-Loop	Feasibility-Enforcing	Adaptive Iterative
Scenario Loop	None (One-shot)	Feasibility Loop Only	**Dual Loop**: Economy & Feasibility
Typical Scenario	**Static**: Pre-fixed based on boundary conditions	**Static**: Pre-fixed based on boundary conditions	**Adaptive**:Updated based on operational states
Extreme Scenario	**Static**: Pre-fixed based on boundary conditions	**Batch**: Iteratively add all infeasible scenarios of operation simulation	**Targeted**: Iteratively add worst-case based on physical indicators
Efficiency	**High** (Small, fixed set)	**Low** (Redundant set)	**Balanced** (Compact set)
MAIG Applicability	**Low** (Infeasible planning schemes in extreme scenarios)	**Limited** (Inefficient due to redundant scenario constraints)	**High** (Coordinated balance of economy, security, and efficiency)

V. CASE STUDY

The effectiveness of the proposed method is evaluated on a modified RTS-GMLC system. The original system contains three areas connected by five inter-area tie lines. In this study, all AC inter-area tie lines are replaced with HVDC links, and electrochemical storage equal to 10% of the installed wind–solar capacity is added. The resulting three-area asynchronous system features distinct renewable resources and load levels across regions, while the HVDC links enable coordinated power interchange.

To validate the performance, four methods are compared. M1 considers only typical scenarios generated by the approach in Section III-A, while M2 incorporates both typical and extreme scenarios in Section III-A. These two methods are compared with two iterative frameworks: M3 is the iterative feasibility-enforcing method in [7], and M4 is the dual-loop adaptive iterative method proposed in this study.

The planning results of different methods are shown in Table III. M1 and M2 have shorter computation time because they do not perform full-year operation simulation, but both result in planning schemes with infeasible scenarios. In contrast, M3 and M4 incorporate the operation simulation, ensuring feasibility with increased computation time, illustrating a tradeoff between efficiency and feasibility. However, as feasibility is indispensable for practical planning applications, the solutions provided by M3 and M4 are more meaningful.

The convergence performance of M4 is shown in Fig. 3. To ensure feasibility, M4 invests more in thermal units, storage and transmission capacity, resulting in higher total cost than

979-8-3315-8138-1

TABLE III
PLANNING RESULTS OF DIFFERENT METHODS

Method	M1	M2	M3	M4
Objective (million CNY)	12237	12422	12784	12697
Annualized investment (million CNY)	3012	3129	3346	3288
Thermal capacity (MW)	1400	1600	1900	1750
Renewable capacity (MW)	6130	6492	6820	6730
Storage capacity (MW)	1004	1017	1245	1180
Transmission line expansion (MW)	435.5	382.9	502.3	468.7
Iteration number	–	–	2	3
Computation time (s)	615.6	4827.7	12945.3	8142.6
Number of infeasible scenarios	7	2	0	0
Relative error of operational cost (%)	10.8	-7.3	-4.4	-1.9

M1 and M2. Compared with M3, M4 adopts a more targeted strategy to select extreme scenarios and obtains a more representative set. As a result, it converges after only three iterations with just two added extreme scenarios, which is slightly slower than M2. In contrast, M3 requires six extreme scenario additions at one iteration, leading to longer computation time. With typical scenarios updated through multiple iterations, M4 also achieves stronger economic representativeness, yielding a smaller error between its representative operational cost and actual operational cost than M1-M3.

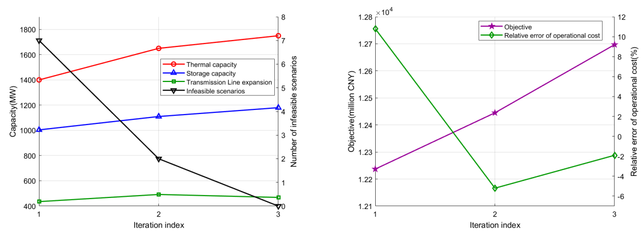

(a) Installed capacity and number of infeasible scenarios.
(b) Objective and relative error of operational cost.

Fig. 3. Convergence performance of the proposed method.

The operation results of the two extreme scenarios extracted during the iteration of M4 are presented in Fig. 4. These two scenarios reflect distinct operating conditions. The scenario of Fig. 4(a) corresponds to a summer peak-load situation with very high demand and low wind output. This leads to a high sustained low renewable output indicator, reflecting the system's prolonged reliance on thermal units during such periods. In contrast, the scenario of Fig. 4(b) features abundant renewable availability, which significantly constrains the operating space for thermal units, reducing online thermal capacity and weakening system flexibility. Consequently, the short-term reserve adequacy and transient frequency security indicators rise, reflecting tighter reserve margins and greater frequency security challenges. These observations show that the proposed scenario extraction method captures multiple dimensions of system stress and reliably identifies representative extreme scenarios, enhancing the robustness of planning.

VI. CONCLUSION

This paper proposes an iterative planning method with dual-loop adaptive representative scenario update to address the challenges of large-scale MAIGs. The method couples

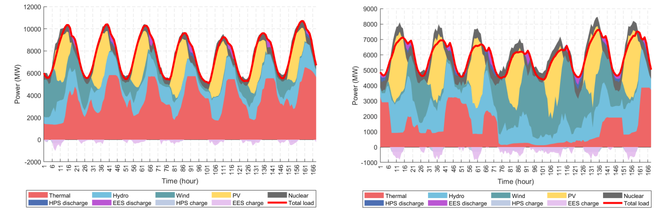

(a) Extreme scenario extracted in the 1st iteration.
(b) Extreme scenario extracted in the 2nd iteration.

Fig. 4. The operation results of the extreme scenarios extracted by the proposed method.

the co-optimized generation–transmission–storage planning model with operation simulation, and updates typical and extreme scenarios through operational-state-based clustering and physics-based indicators defined over multiple time scales. By iteratively feeding refined scenarios back into planning with a dual-loop mechanism, the method captures both diverse operational patterns and feasibility-critical extreme conditions that fixed-scenario methods overlook. The case study on a modified RTS-GMLC system shows that the proposed method achieves a balance between economy, security, and computational efficiency, demonstrating its value for long-term planning of MAIGs.

REFERENCES

[1] X. Zhang and A. J. Conejo, "Coordinated investment in transmission and storage systems representing long-and short-term uncertainty," *IEEE Transactions on Power Systems*, vol. 33, no. 6, pp. 7143–7151, 2018.
[2] F. Verástegui, A. Lorca, D. E. Olivares, M. Negrete-Pincetic, and P. Gazmuri, "An adaptive robust optimization model for power systems planning with operational uncertainty," *IEEE Transactions on Power Systems*, vol. 34, no. 6, pp. 4606–4616, 2019.
[3] K. Poncelet, H. Höschle, E. Delarue, A. Virag, and W. D'haeseleer, "Selecting representative days for capturing the implications of integrating intermittent renewables in generation expansion planning problems," *IEEE Transactions on Power Systems*, vol. 32, no. 3, pp. 1936–1948, 2016.
[4] M. Zatti, M. Gabba, M. Freschini, M. Rossi, A. Gambarotta, M. Morini, and E. Martelli, "k-milp: A novel clustering approach to select typical and extreme days for multi-energy systems design optimization," *Energy*, vol. 181, pp. 1051–1063, 2019.
[5] Á. García-Cerezo, R. García-Bertrand, and L. Baringo, "Enhanced representative time periods for transmission expansion planning problems," *IEEE Transactions on Power Systems*, vol. 36, no. 4, pp. 3802–3805, 2021.
[6] A. Yeganefar, M. R. Amin-Naseri, and M. K. Sheikh-El-Eslami, "Improvement of representative days selection in power system planning by incorporating the extreme days of the net load to take account of the variability and intermittency of renewable resources," *Applied Energy*, vol. 272, p. 115224, 2020.
[7] H. Teichgraeber, C. P. Lindenmeyer, N. Baumgärtner, L. Kotzur, D. Stolten, M. Robinius, A. Bardow, and A. R. Brandt, "Extreme events in time series aggregation: A case study for optimal residential energy supply systems," *Applied energy*, vol. 275, p. 115223, 2020.
[8] P. Wang, E. Du, N. Zhang, X. Xu, and Y. Gao, "Power system planning with high renewable energy penetration considering demand response," *Global Energy Interconnection*, vol. 4, no. 1, pp. 69–80, 2021.
[9] Q. Shi, F. Li, and H. Cui, "Analytical method to aggregate multi-machine sfr model with applications in power system dynamic studies," *IEEE Transactions on Power Systems*, vol. 33, no. 6, pp. 6355–6367, 2018.
[10] H. Jiang, E. Du, B. He, N. Zhang, P. Wang, F. Li, and J. Ji, "Analysis and modeling of seasonal characteristics of renewable energy generation," *Renewable Energy*, vol. 219, p. 119414, 2023.

979-8-3315-8138-1